

# Large Scale Business Store Front Detection from Street Level Imagery

Qian Yu, Christian Szegedy, Martin C. Stumpe,  
Liron Yatziv, Vinay Shet, Julian Ibarz, Sacha Arnoud  
Google StreetView

qyu, szegedy, mstumpe, lirony, vinayshet, julianibarz, sachaa@google.com

## Abstract

We address the challenging problem of detecting business store fronts in street level imagery. Business store fronts are a challenging class of objects to detect due to high variability in visual appearance. Inherent ambiguities in visually delineating their physical extents, especially in urban areas, where multiple store fronts often abut each other, further increases complexity. We posit that traditional object detection approaches such as those based on exhaustive search or those based on selective search followed by post-classification are ill suited to address this problem due to these complexities. We propose the use of a Multibox [4] based approach that takes as input image pixels and directly outputs store front bounding boxes. This end-to-end learnt approach instead preempts the need for hand modelling either the proposal generation phase or the post-processing phase, leveraging large labelled training datasets. We demonstrate our approach outperforms the state of the art detection techniques with a large margin in terms of performance and run-time efficiency. In the evaluation, we show this approach achieves human accuracy in the low-recall settings. We also provide an end-to-end evaluation of business discovery in the real world.

## 1. Introduction

The abundance of geo-located street level photographs available on the internet today provides a unique opportunity to detect and monitor man-made structures to help build precise maps. One example of such man-made structures is local businesses such as restaurants, clothing stores, gas stations, pharmacies, laundromats, etc. There is a high degree of consumer interest in searching for such businesses through local queries on popular search engines. Accurately identifying the existence of such local businesses worldwide is a non-trivial task. We attempt to automatically identify a business by detecting its presence on geo-located street level photographs. Specifically, we explore the world’s largest archive of geo-located street level pho-



Figure 1: Typical Street View image showing multiple store fronts. The red boxes show successfully detected store fronts using the approach presented in this paper

tos, Google Street View [23, 1], to extract business store fronts. Figure 1 illustrates our use case and shows sample detections using the approach presented in this paper.

Extracting arbitrary business store fronts from Street View imagery is a hard problem. Figure 2 illustrates some of the challenges. The complexity comes from the high degree of intra-class variability in the appearance of store fronts across business categories and geographies (Figure 2 a-d), inherent ambiguity in the physical extent of the store front (Figure 2 d-e), businesses abutting each other in urban areas, and the sheer scale of the occurrence of store fronts worldwide (likely in the hundreds of millions). These factors make this an ambiguous task even for human annotators. Image acquisition factors such as noise, motion blur, occlusions, lighting variations, specular reflections, perspective, geo-location errors, *etc.* further contribute to the complexity of this problem. Given the scale of this problem and the turn over rate of businesses, manual annotation is prohibitive and unsustainable. For automated approaches, runtime efficiency is highly desirable for detecting businesses worldwide in a reasonable time-frame.

Detecting business store fronts is the first and most crit-



Figure 2: Precisely detecting business is a challenging task. The top row illustrates the large variance between different categories. The bottom row shows business boundary is difficult to precisely define.

ical step in a multi-step process to extract usable business listings from imagery. Precise detection of store fronts enables further downstream processing such as geo-location of the store front, extraction of business names and other attributes, e.g. category classification. In this paper, we focus on this critical first step, namely, precisely detecting business store fronts at a large scale from StreetView imagery.

In this paper, we propose a Convolutional Neural Network (CNN) based approach to large scale business store front detection. Specifically, we propose the use of the MultiBox [4] approach to achieve this goal. The Multi-box approach uses a single CNN to take image pixels as input and directly predict bounding boxes, corresponding to the object of interest, together with their confidences. The inherent ambiguities in delineating store fronts and their tendency to abut each other in urban areas provides a challenge to traditional object detection approaches such as those based on exhaustive search or those based on selective search followed by a post-classification stage. In this paper, we have a comparative study to show that the end-to-end fully learned Multibox approach outperforms traditional object detection approaches both in accuracy and in run-time efficiency, enabling automatic business store front detection at scale.

In our comparison with other two approaches, Selective Search [22] and Multi-Context Heatmap [16], we found that the head on approach of Multibox attacking the detection problem directly improves the quality of results while reducing the engineering effort. Selective search is designed specifically for natural objects, so its coverage is inferior

for store fronts which require very subtle visual cues to be separated. On the other hand, heatmap based approaches like [21] and [16] do not produce bounding boxes directly, but need to post-process some intermediate representation: heatmaps produced by convolutional networks. This incurs extra engineering effort in the form of an additional step that needs to be optimized for new use cases. In contrast, MultiBox learns to produce the end result directly by the virtue of a single objective function that can be optimized jointly with the convolutional features. This eases adaptation to a specific domain. Also, the superior quality of the solution comes with a significant reduction of computational cost due to extensive feature sharing between the confidence and regression computations for a large number of object proposals simultaneously.

## 2. Related Work

The general literature on image understanding is vast. Object classification and detection [6] has been driven by the Pascal VOC object detection benchmark [8] and more recently the ImageNet Large Scale Visual Recognition Challenge (ILSVRC) [5]. Here, we focus on reviewing related work on analyzing Street View data, object detection and the use of Deep Convolutional Networks.

**Analyzing Street View Data.** Since its launch in 2007, Google Street View [23, 1] has been used by the computer vision community as both a test bed for algorithms [15, 24] and a source from which data is extracted and analyzed [9, 25, 17, 2].

Early work on leveraging street level imagery focused on 3D reconstruction and city modeling, such as in [2, 17]. Later works have focused on extracting knowledge from Street View and leveraging it for particular tasks. In [25] the authors presented a system in which SIFT descriptors from 100,000 Street View images were used as reference data to be queried upon for image localization. Xiao *et al.* [24] proposed a multi view semantic segmentation algorithm that classified image pixels into high level categories such as ground, building, person, etc. Lee *et al.* [15] described a weakly supervised approach that mined mid-level visual elements, and their connections in geographic datasets. Most similar to our work, is that of Goodfellow *et al.* [9]. Both work utilizes Street View as a map making source, and data mine information about real world objects. They focus on understanding street numbers, while we are concerned with local businesses. They specifically describe a method for street number transcription in Street View data. Their approach unified the localization, segmentation, and recognition steps by using a Deep Convolutional Network that operates directly on image pixels. Their method, which was evaluated on tens of millions of annotated street number images from Street View, achieved above 90% accuracy and was comparable to human operator precisions at a coverage

above 89%.

**Convolutional Networks.** Convolutional Networks [7, 14] are neural networks that contain sets of nodes with tied parameters. Increases in size of available training data and availability of computational power, combined with algorithmic advances such as piecewise linear units [12, 10] and dropout training [11] have resulted in major improvements in many computer vision tasks. Krizhevsky et al. [13] showed a large improvement over the state of the art in object recognition. This was later improved upon by Zeiler and Fergus [26], and Szegedy et al. [19].

On immense datasets, such as those available today for many tasks, overfitting is not a concern; increasing the size of the network provides gains in testing accuracy. Optimal use of computing resources becomes a limiting factor. To this end Dean et al. developed DistBeleif [3], a distributed, scalable implementation of Deep Neural Networks. We base our system on this infrastructure.

**Object Detection.** Traditionally, object detection is performed by exhaustively searching for the object of interest in the image. Such approaches produce a probability map corresponding to the existence of the object at a location. Post-processing of this probability map, either through non-maxima suppression or mean-shift based approaches, then generates discrete detection results. To counter the computational complexity of exhaustive search, selective search [22] by Uijlings et al. uses image segmentation techniques to generate several proposals drastically cutting down the number of parameters to search over. Girshick et al proposed R-CNN [8] which uses a convolutional post-classifier network to assign the final detection scores. The MultiBox by Erhan et al. [4] takes this approach even further by adopting a fully learnt approach from pixels to discrete bounding boxes. The end-to-end learnt approach has the advantage that it integrates the proposal generation and post-processing using a single network to predict a large number of proposals and confidences at the same time. Although MultiBox can produce high quality results by relying on the confidence output of the MultiBox network alone, the precision can be pushed further by running extra dedicated post-classifier networks for the highest confidence proposals. Even with the extra post-classification stage, the MultiBox approach can be orders of magnitude faster than R-CNN depending on the desired recall.

### 3. Proposed Approach

Most state-of-the-art object detection approaches utilize a proposal generation phase followed by a postclassification pass. In our case, traditional hand-crafted saliency based proposal generation methods have two fundamental issues. First of all, our images are very large and detailed, so we end up with a very large number (on average 4666) of proposals per panorama. This makes the postclassification pass very

expensive computationally at the required scale. Secondly, the coverage of the selective search [22] based proposals at 0.5 overlap is only 62%. We hypothesize that this is due to the fact that the boundaries between businesses require the utilization of much more subtle clues to be separated from each other than large, clearly disjoint natural objects.

The large amount of training data makes this task a prime candidate for the application of some learned proposal generation approach. MultiBox was introduced in [4] and stands out for this task given its relative modest computational cost and its high detection quality on natural images [20].

#### 3.1. MultiBox

The general idea of MultiBox [4] is to use a single convolutional network evaluation to directly predict multiple bounding box candidates together with their confidence scores. MultiBox achieves this goal by using a precomputed clustering of the space of possible object locations into a set of  $n$  “priors”. The output of the convolutional network is  $5n$  numbers: the  $4n$ -dimensional “location output” (four values for each prior) and the  $n$ -dimensional “confidence output” (one value for each prior). These  $5n$  numbers are predicted by a linear layer fully connected to the  $7 \times 7$  grid of the Inception module described in [20] for which the filter sizes of that module are reduced to 64 (32 in the  $1 \times 1$  and  $3 \times 3$  convolutional layers each). This is necessary to constrain the number of parameters; for example, 12.5 million for  $n = 800$  priors.

The priors have double purpose. During training time, the priors are matched with the ground-truth boxes  $g_j$  via maximum weight matching, where the edge weight between box  $g_j$  and prior  $p_i$  is their Jaccard overlap. Let  $(x_{ij})$  denote the adjacency matrix of that matching: that is  $x_{ij} = 1$  if ground-truth box  $j$  was matched with prior  $i$ .  $x_{ij} = 0$  for all other pairs of  $(i, j)$ . Note that  $x_{ij}$  is independent of the network prediction, it is computed from the ground-truth locations and priors alone. During training, the location output  $l'_i$  of the network for slot  $i$  (relative to the prior) should match the ground-truth box  $g_j$  if the ground-truth box  $g_j$  was matched with prior  $i$  (that is if  $x_{ij} = 1$ ). Since the network predicts the location  $l'_i$  relative to  $i$ -th prior, we set  $l_i = l'_i + p_i$  which is the prediction of ground-truth location  $g_j$ , when  $i$  is matched with  $j$ . The target for the logistic confidence output  $i$  is 1 in this case and is set to 0 for all priors that are not matched with any ground-truth box. The overall MultiBox loss is then given by:

$$\sum_{i,j} x_{ij} \left( \frac{\alpha}{2} \|l_i - g_j\| - \log(c_i) \right) - \sum_i (1 - \sum_j x_{ij}) \log(1 - c_i),$$

which is the weighted sum of the  $L_2$  localization loss and the logistic loss for the confidences. We have tested various values of  $\alpha$  on different data-sets and based on those

experiments, we have used  $\alpha = 0.3$  in this setup as well.

This scheme raises the question of whether we should pick specialized prior for this task. However, we found that any set of prior that covers the space of all rectangles (within a reasonable range of size and aspect ratios) results in good models when used for training. Therefore, in our setting, we reused the same set of 800 priors that were derived from clustering all the objects in the ILSVRC 2014 dataset. Given the qualitatively tight inferred bounding boxes from our results, we do not expect significant gains from using a different set of priors specifically engineered for this task.

Furthermore, the fact that bounding boxes of businesses do not tend to overlap means that the danger of two store fronts matching the exact same prior is much lower than for natural objects that can occur in cluttered scenes in highly overlapping positions. Also the low probability of overlap allows for applying non-maximum suppression with a relatively low overlap threshold of 0.2. This cuts the number of boxes that need to be inspected in the post-classification pass significantly.

The quality of MultiBox can be significantly enhanced by applying it in a very coarse sliding window fashion: we have used three scales with a minimum overlap of 0.2 between adjacent tiles, which ends up with only 87 crops in total for an entire panorama. In the following, this approach will be referred to as *multi-crop evaluation*. For detecting objects in natural web images, single crop evaluation works well with MultiBox, but since our panoramas are high resolution, smaller businesses cannot be reliably detected from a low resolution version of a single panorama. However, if the proposals coming from the various crops are merged without postprocessing, businesses not fully contained in one crop tend to get detected with high confidence and suppress the more complete views of the same detection. To combat this failure mode, we need to drop every detection that abuts one of the edges of the tile, unless that side also happens to be a boundary of the whole panorama. After multi-crop evaluation, we first drop the proposals that are below a certain threshold and then drop the ones that are not completely contained in the (0.1, 0.1) - (0.9, 0.9) sub-window of the crop. A non-maximal suppression is applied to combine all of the generated proposals. There is not any preprocessing in terms of geometry rectification or masking out sky or ground regions.

### 3.2. Postclassification

We found that postclassification could increase the average precision of the detections by 6.9%. For this reason, we trained a GoogLeNet [19] model and applied it in the R-CNN manner described in [8]: i.e. extending the proposal by 16.6% and applying an affine transformation it to the  $224 \times 224$  receptive field of the network. For any given box in an image  $I$ , let  $B(b)$  denote the event that box  $b$  over-

laps the bounding box of a business with at least 0.5 Jaccard overlap. Our task is to estimate  $P(B(b)|I)$  for all proposals produced by the MultiBox. This probability can be computed by marginalizing over each detection  $b_i$  that has at least 0.5 overlap with  $b$ :

$$P(B(b)|I) = \sum_{b_i} P(B(b)|D(b_i))P(D(b_i)|I),$$

where  $D(b_i)$  is the event that multibox detects  $b_i$  in the image. This suggests that the probability that box  $b$  corresponds to a business can be estimated by a sum of products of the confidence scores  $\sum S_p(b)S_d(b_i)$  with all boxes  $b_i$  overlapping  $b$  with Jaccard similarity greater than 0.5, where  $S_p$  and  $S_d$  denotes the score of postclassifier and that of the MultiBox detector network, respectively. In practice however, we used non-maximum suppression with the very low threshold of 0.2 on top of the detected boxes leaving us with a single term in the above sum:  $S_p(b)S_d(b)$ , which is simply the product of the scores of the MultiBox network and the postclassifier network for box  $b$ . This is in fact the final score used for ranking our detections at evaluation time.

### 3.3. Training Methodology

Both the MultiBox and postclassifier networks were trained with the DistBelief [3] machine learning system using stochastic gradient descent. For Panorama images, we downsized the original image by a factor of 8 for training both the MultiBox and the post-classifier networks. The postclassifier network was trained with random mixture of positive and negative crops in 1:7 ratio. The negative crops were generated with MultiBox output with a low confidence threshold.

### 3.4. Detection in Panorama Space

To avoid the loss of recall due to restriction of field of view, we detect business store fronts in panorama space. Street View panoramas are created by projecting individual camera images onto a sphere and stitching them together. The resulting panorama image is represented in equirectangular projection, i.e. the spherical image is projected onto a plane with  $360^\circ$  along the horizon and  $90^\circ$  up and  $90^\circ$  down as shown in Figure 3. Each camera image only has a relatively small field-of-view, which makes business detection in the individual camera images not feasible since camera images often cut through store fronts as shown in Figure 3. Hence, our approach is trained and tested on the equirectangular panoramas. As compared to single camera images, this image representation has the disadvantage of having the equirectangular distortion pattern. Experiments show that the Deep Convolutional Network is able to learn the store front detection even under this distortion.

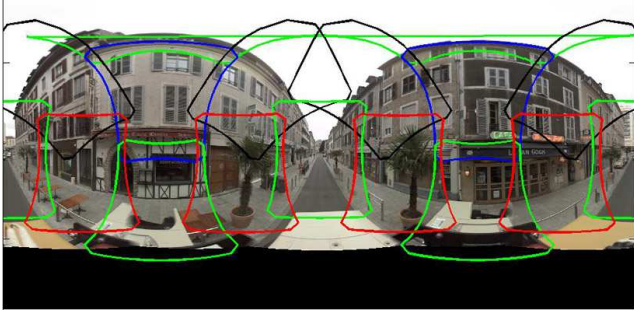


Figure 3: StreetView panoramas are composed of multiple individual images (outlined in colors) which are projected to a sphere and blended together represented as a 2D equirectangular projection.

## 4. Results

In this section we present our empirical results. First, we describe how training and testing datasets are prepared. Next, we present the evaluation procedure and compare our approach with other state of the art object detection approaches. Finally, we have an end-to-end evaluation of the overall business discovery results in the real world. Some qualitative detection results in panorama space are shown at the end of paper.

### 4.1. Business Store Front Dataset

There is no large scale business store front dataset available publicly. We have labeled about 2 million panorama images in more than 12 countries. Annotations for this dataset were done through a crowd-sourcing system. The original resolution of panorama image is 13312x6656. For most of the business store fronts, the width varies from 200 to 2000 and the aspect ratio varies from 1/5 to 5/1.

Since businesses can be imaged multiple times from different angles, the splitting between training and testing is location aware, similar to the one used in [18]. This ensures that businesses in the test set were never observed in the training set.

Similar to most object annotation tasks, it is hard to enforce the completeness of the annotation, especially at this scale. In order to have a proper evaluation on this problem, we sub-sampled a smaller test dataset with 2,000 panorama images, where we enforce the completeness of annotations by increasing operator replication and adding a quality control stage in the crowd-sourcing system to ensure all visible businesses from the panoramas are labeled with the best effort. Compared to the original 2934 store front annotations in the original test set, about 11,000 annotations were created. This indicates how incomplete the training dataset is. We use this smaller but more complete dataset as the test set

for comparison.

### 4.2. Runtime Quality Tradeoff

Computational efficiency is a major objective for large scale object detection. In this section, we analyse the trade-off between runtime efficiency and detection quality. For our approach, the computational cost is determined by the number of crops (*i.e.* number of MultiBox evaluations) and the number of proposals generated by MultiBox (*i.e.* number of post-classification evaluations). We adopt Average Precision (AP) as the overall quality metric. For automatic business discovery, it is more important to have high precision results.

Compared to the objects in Imagenet detection task, business store fronts are relatively small in the entire panorama. The single crop setting [20] does not apply to our problem, at least not with the 224x224 receptive field size used for training this network. We have to apply the MultiBox model at different locations and different scales, *i.e.* do a multi-crop evaluation. It is worth noting that the multi-crop evaluation is different from the classic sliding window approach since the crop does not correspond to the actual store front. Figure 4 (a) shows AP increases (from 0.304 to 0.358) while the number of crops increases (from 69 to 904). However, AP improvement is mostly due to the increase of recall at low precision area. Figure 4 (b) shows three Precision-Recall curves at different number of crops. There is a minor performance loss at the high precision area with fewer crops.

After MultiBox evaluation, we use a fixed threshold to select proposals for post-classification. A lower threshold will generate more proposals. Figure 4 (c) shows performance of AP varies as the number of proposals on average per image increases. We select a threshold that generates about 37 proposals on average per panorama, which gives the best performance. We did notice that, the performance starts to degrade if we generate too many proposals.

### 4.3. Comparison with Selective Search

Here we compare with Selective Search in term of both accuracy and runtime efficiency. We first tuned the Selective Search parameters to get a max recall of 62% with 4666 proposals per image. For comparison, MultiBox achieve 91% recall with only about 863 proposals per image. A bigger number of selective search proposals per image starts to hurt AP.

MultiBox’s post-classification model is only trained with MultiBox output with a low threshold, which allows MultiBox to propose more boxes to ensure we have enough negative samples while training post-classification. A separate post-classification model is trained for Selective Search boxes. Both models are initialized from ILSVRC classification challenge task. Figure 5 shows comparison be-

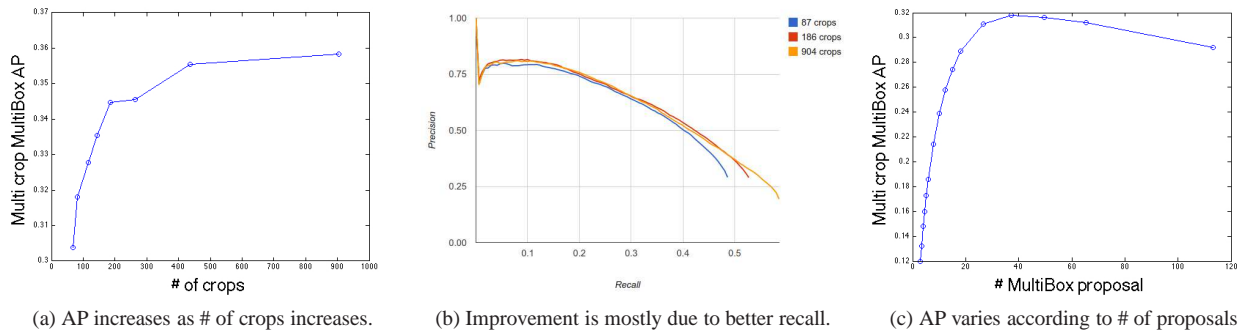


Figure 4: Runtime quality tradeoff.

tween several approaches. The MultiBox result alone outperforms Selective Search + Post-Classification with a significant margin. Moreover, the computational cost of our approach is much lower, roughly  $1/37$  ( $= \frac{37+87}{4666}$ ), than Selective Search+postclassification. Given a rate of 50 images/second using one network evaluation on a current Xeon workstation<sup>1</sup>, this means 2.5 seconds per panorama for our approach as opposed to 1.5 minutes per panorama for Selective Search+post-classification.

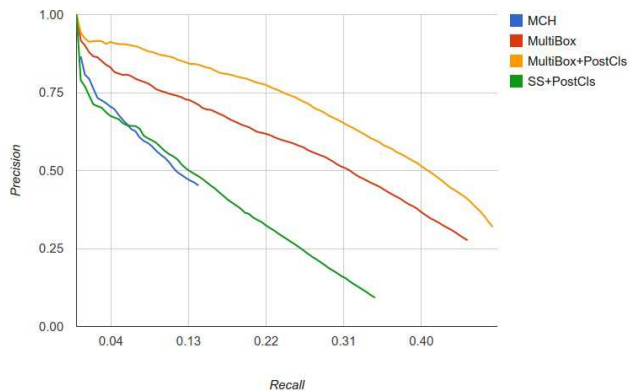


Figure 5: Comparison between MultiBox, MultiBox + Post-Classification, Selective Search (SS) + Post-Classification and Multi-Context Heatmap (MCH).

#### 4.4. Comparison with Trained Heat Map Approach

In this section, we compare with another Deep Neural Network base object detection approach in [16], Multi-Context HeatMap (MCH). Similar to [21], this approach adopts an architecture that outputs a heatmap instead of

a single classification value. The main difference of [16] compared to [21] is that it uses a multi-tower convolutional that is fed different resolutions of the image to get more context information as well as the loss being a simple logistic regression loss instead of the L2 error minimization proposed in [21], which is more discriminative at the pixel level. A model-free post-processing is used to convert the heatmap to detection results. This approach has been successfully applied in several detections tasks, such as text detection, street sign detection where the overall accuracy of the model was reaching human operator labels or was close to it [16]. MultiBox significantly outperforms MCH in the business detection case. Figure 6 illustrates the comparison with MCH on one example. Although the heatmap (Figure 6 (b)) generated by MCH is quite meaningful, converting the heatmap to actual detection windows is a non-trivial task. Figure 6 (c) shows the detection windows generated by the post-processing. One can always try different post-processing algorithms. However, such not learning based post-processing algorithms may either over-segment or under-segment business store fronts from the heatmap. Compared to MultiBox, the MCH model is much more sensitive to label noise present in the training set. Moreover, since the cost function is at the pixel level, the MCH model will have the same penalty on the errors on an border of an object as on the error far from the border. Thus, it has difficulty to predict the precise boundary. One reason why MCH works so well on other applications, such as traffic signs and text, is probably because the boundary definition of these objects is very well defined and consistent and the objects do not adjoin each other as business store fronts.

#### 4.5. Comparison with Human Performance

Besides the obvious scalability issues, there are a lot of cases in which human annotators disagree with each other due to ambiguity in business boundaries. We have sent human annotated store fronts and auto detected store fronts to

<sup>1</sup>Intel(R) Xeon(R) CPU E5-1650 0 @ 3.20GHz, memory 32G.

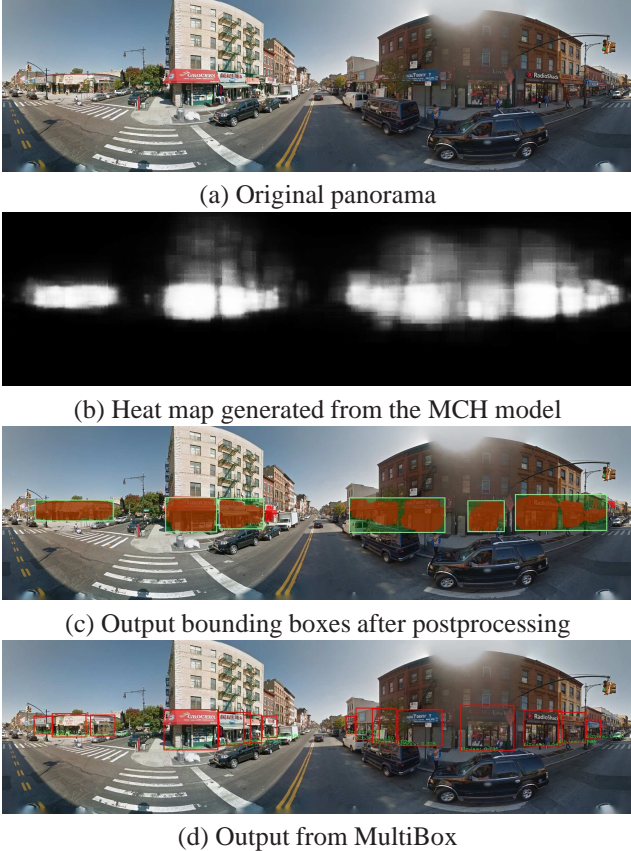


Figure 6: Compare MultiBox with Multi-Context Heatmap

human annotators to let them decide whether the box is a store front. Each question was sent to three different annotators who have been trained for annotating business store fronts. They did not know if a box has been generated by the detector or human annotators. A box was confirmed as a true positive if two or more positive answers were received. We used two different sets of human annotations: one from the original annotation effort, where we do not enforce the completeness of the annotation, the other one from the new annotation effort, where we enforced the completeness of the annotation. We called the first one “Human Low-Recall” set and the second one “Human High-Recall” set. The comparison is shown in Table 1. It turns out for both annotation efforts, humans only achieve a precision below 90%. In other words, on more than 10% of the annotations human could not agree with each other. This indicates the ambiguity of labeling the business store fronts. Given that humans may miss annotations as well, it is hard to get true recall. So we use “Box Per Image” as an alternative indicator of coverage. At the same precision (89.50%), the detector already achieves slightly higher Box Per Image than human annotators in low recall mode. Moreover, the detector gives us the

flexibility to select an operating point at higher precision.

	Precision	Box Per Image
Human Low-Recall	89.50%	<b>1.467</b>
Human High-Recall	88.72%	5.531
<b>Auto Detector</b>	89.50%	<b>1.471</b>
	92.00%	1.063

Table 1: Comparison with human annotation

Although the precision of the MultiBox detector is measured to be higher than that of human annotators at some operating points, we notice that it tends to generate more egregious false positives than humans did. Figure 7 shows some of the false positives generated by the detector. Humans are unlikely to make mistakes such as in Figure 7 (a) and (b). However, business advertisement sign shown in Figure 7 (c) looks so similar to a business store front that can be confusing to human annotators.

#### 4.6. Business Discovery End-to-End Evaluation

We used auto detector to generate tens of millions business store front detections. It is hard to understand actual business coverage by comparing with the ground truth in the image space. Given business store front detections from multiple images, we first merge detections at the same location with a geo-clustering process. This helps us to remove some of the remaining false positives, *e.g.* business names on vehicles. GIS information can also help us to further remove false positives, such as those on high ways, or in residential areas. Although the complete end-to-end system is out of the scope of this paper, we would like to provide a better understanding of the coverage of our automated business discovery process in terms of precision and recall in the real world.

For this reason, we conducted a small scale exhaustive end-to-end evaluation in Brazil. We selected a metro area of about one square kilometre and let annotators have a Street View virtual walk and count all visible businesses. In total, 931 unique business were found by this manual process. Simultaneously, we let annotators verify the automatically detected businesses within the same region before geo-clustering. Each automatically detected business in the area was sent to three operators and was considered a true positive if two or more confirmations were received. The automatic detector achieved 94.6% precision: it got 56 false positives out of the 1045 detections. Then, we applied geo-clustering to remove the duplicate geo-locations from the list of the detections resulting in 495 unique businesses. This means a **53.2%** recall at **94.6%** precision: 495 out of 931 businesses visible on Street View imagery were correctly detected by our automatic system.

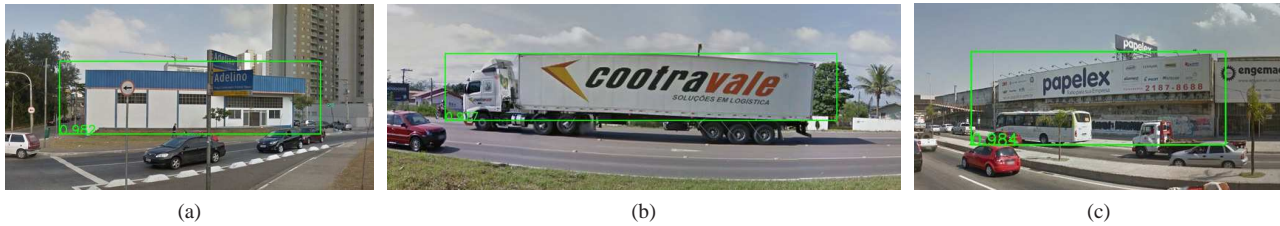


Figure 7: Some typical false positives of detection results



Figure 8: Qualitative detection results in panorama space.

## 5. Summary

In this paper, we propose to use MultiBox to detect business store fronts at scale. Our approach outperforms two other successful detection techniques by a large margin. The computational efficiency of our approach makes the large scale business discovery worldwide possible. We also compare the detector performance with human performance and show that human operators tend to agree more with the detector’s output than with human annotations. Finally, we conducted an end-to-end evaluation to demonstrate the coverage in physical space. Given the high computational efficiency of the current detector, in order to further improve the detector’s performance, we will investigate on using more context features for postclassification and larger networks.

## References

[1] D. Anguelov, C. Dulong, D. Filip, C. Frueh, S. Lafon, R. Lyon, A. Ogale, L. Vincent, and J. Weaver. Google street view: Capturing the world at street level. *Computer*, 2010. 1, 2

[2] N. Cornelis, B. Leibe, K. Cornelis, and L. Van Gool. 3d urban scene modeling integrating recognition and reconstruction. *International Journal of Computer Vision*, 2008. 2

[3] J. Dean, G. Corrado, R. Monga, K. Chen, M. Devin, M. Mao, M. aurelio Ranzato, A. Senior, P. Tucker, K. Yang, Q. V. Le, and A. Y. Ng. Large scale distributed deep networks. In F. Pereira, C. Burges, L. Bottou, and K. Weinberger, edi-

tors, *Advances in Neural Information Processing Systems 25*, pages 1223–1231, 2012. 3, 4

[4] D. Erhan, C. Szegedy, and D. Anguelov. Scalable object detection using deep neural network. In *In Computer Vision and Pattern Recognition (CVPR), 2014 IEEE Conference on*, pages 2155–2162, 2014. 1, 2, 3

[5] M. Everingham, L. Van Gool, C. K. I. Williams, J. Winn, and A. Zisserman. The PASCAL Visual Object Classes Challenge 2011 (VOC2011) Results. <http://www.pascal-network.org/challenges/VOC/voc2011/workshop/index.html>. 2

[6] P. F. Felzenszwalb, R. B. Girshick, D. McAllester, and D. Ramanan. Object detection with discriminatively trained part based models. *IEEE Transactions on Pattern Analysis and Machine Intelligence (PAMI)*, 2010. 2

[7] K. Fukushima. Neocognitron: A self-organizing neural network model for a mechanism of pattern recognition unaffected by shift in position. *Biological cybernetics*, 36(4), 1980. 3

[8] R. Girshick, J. Donahue, T. Darrell, and J. Malik. Rich feature hierarchies for accurate object detection and semantic segmentation. In *Proceedings of the IEEE Conference on Computer Vision and Pattern Recognition (CVPR)*, 2014. 3, 4

[9] I. J. Goodfellow, Y. Bulatov, J. Ibarz, S. Arnaud, and V. Shet. Multi-digit number recognition from street view imagery using deep convolutional neural networks. *arXiv preprint arXiv:1312.6082*, 2013. 2

[10] I. J. Goodfellow, D. Warde-Farley, M. Mirza, A. Courville, and Y. Bengio. Maxout networks. *arXiv preprint arXiv:1302.4389*, 2013. 3

- [11] G. E. Hinton, N. Srivastava, A. Krizhevsky, I. Sutskever, and R. R. Salakhutdinov. Improving neural networks by preventing co-adaptation of feature detectors. *arXiv preprint arXiv:1207.0580*, 2012. 3
- [12] K. Jarrett, K. Kavukcuoglu, M. Ranzato, and Y. LeCun. What is the best multi-stage architecture for object recognition? In *Computer Vision, 2009 IEEE 12th International Conference on*. IEEE, 2009. 3
- [13] A. Krizhevsky, I. Sutskever, and G. E. Hinton. Imagenet classification with deep convolutional neural networks. In *Advances in neural information processing systems*, 2012. 3
- [14] Y. LeCun, L. Bottou, Y. Bengio, and P. Haffner. Gradient-based learning applied to document recognition. *Proceedings of the IEEE*, 86(11), 1998. 3
- [15] Y. J. Lee, A. A. Efros, and M. Hebert. Style-aware mid-level representation for discovering visual connections in space and time. In *Computer Vision (ICCV), 2013 IEEE International Conference on*, 2013. 2
- [16] Anonymized for review. Fast and reliable object detection using multi-context deep convolutional network. Unpublished, 2015. 2, 6
- [17] B. Micusik and J. Kosecka. Piecewise planar city 3d modeling from street view panoramic sequences. In *Computer Vision and Pattern Recognition, 2009. CVPR 2009. IEEE Conference on*. IEEE, 2009. 2
- [18] Y. Movshovitz-Attias, M. C. Stumpe, V. Shet, S. Arnaud, and L. Yatziv. Ontological supervision for fine grained classification of street view storefront. In *Computer Vision and Pattern Recognition (CVPR), 2015 IEEE Conference on*, 2015. 5
- [19] C. Szegedy, W. Liu, Y. Jia, P. Sermanet, S. Reed, D. Anguelov, D. Erhan, V. Vanhoucke, and A. Rabinovich. Going deeper with convolutions. *arXiv:1409.4842 [cs]*, sep 2014. 3, 4
- [20] C. Szegedy, S. Reed, D. Erhan, and D. Anguelov. Scalable, high-quality object detection. In <http://arxiv.org/abs/1412.1441>, [v2] Thu, 26 Feb 2015 19:22:26 GMT (132kb,D), 2015. 3, 5
- [21] C. Szegedy, A. Toshev, and D. Erhan. Deep neural networks for object detection. 2013. 2, 6
- [22] J. Uijlings, K. van de Sande, T. Gevers, and A. Smeulders. Selective search for object recognition. *International Journal of Computer Vision*, 2013. 2, 3
- [23] L. Vincent. Taking online maps down to street level. *Computer*, 2007. 1, 2
- [24] J. Xiao and L. Quan. Multiple view semantic segmentation for street view images. In *Computer Vision, 2009 IEEE 12th International Conference on*, 2009. 2
- [25] A. R. Zamir and M. Shah. Accurate image localization based on google maps street view. In *Computer Vision/ECCV 2010*. Springer, 2010. 2
- [26] M. D. Zeiler and R. Fergus. Visualizing and understanding convolutional neural networks. *arXiv preprint arXiv:1311.2901*, 2013. 3